A Smartphone Localization Algorithm Using RSSI and Inertial Sensor Measurement Fusion

William Wei-Liang Li*, *Member, IEEE,* Ronald A. Iltis*, *Senior Member, IEEE,* and Moe Z. Win†, *Fellow, IEEE*

*Department of Electrical and Computer Engineering, University of California, Santa Barbara, CA 93106 USA
†Laboratory for Information and Decision Systems, Massachusetts Institute of Technology, Cambridge, MA 02139 USA

***Abstract*—Indoor navigation using the existing wireless infrastructure and mobile devices is a very active research area. The major challenge is to leverage the extensive smartphone sensor suite to achieve location tracking with high accuracy. In this paper, we develop a navigation algorithm which fuses the WiFi received signal strength indicator (RSSI) and smartphone inertial sensor measurements. A sequential Monte Carlo filter is developed for inertial sensor based tracking, and a radiolocation algorithm is developed to infer mobile location based on RSSI measurements. The simulation results show that the proposed algorithm significantly outperforms the extended Kalman filter (EKF), and achieves competitive location accuracy compared with the round trip time (RTT) based ultra-wideband (UWB) system.**

***Index Terms*—Indoor navigation, smartphone localization, inertial measurement unit (IMU), particle filter, information fusion.**

I. Introduction

Future wireless applications face an increasing demand for location information to enable numerous commercial and public services [1]–[3]. However, navigation in indoor environment is very challenging due to the attenuation of global positioning system (GPS) signals. In recent years, emerging wireless technologies [4]–[6] and advanced filtering techniques [7]–[9] have played a pivotal role in the design of accurate indoor navigation systems.

Smartphones have been incorporating ever more powerful computing capability and sensor functions. The recent smartphones are equipped with an inertial measurement unit (IMU) including accelerometer and gyroscope. These inertial sensors measure the force and angular velocity, which can be exploited to assist navigation when the GPS signal is severely attenuated. However, IMU-based navigation is sensitive to initialization and is only accurate for a short period due to the cubic error drift [10]. Hence, it is usually used with fusion of other measurements, e.g., radiolocation using UWB, Bluetooth, and WiFi [11]–[14].

Radiolocation is a key component of indoor navigation systems, which use the round trip time (RTT) or received signal strength indicator (RSSI) to infer the location. UWB has been considered in RTT-based radiolocation for high accuracy due to its fine signal resolution [5], [15]. However, the high cost of adding UWB to current wireless devices hinders a wide commercial deployment. Hence, it is more desirable to design an indoor navigation system which exploits the existing communication infrastructure and devices. As one of the most common wireless technologies, WiFi is widely available in indoor areas such as offices and shopping malls. Moreover, WiFi RSSI can be easily detected on a smartphone without modifying the physical layer, and hence, greatly facilitates indoor localization and navigation [16]–[18].

In this paper, we develop a location tracking algorithm which fuses the WiFi RSSI and smartphone inertial sensor measurements to track the mobile node position. The major contributions are summarized as follows:

- We design a Sequential Monte Carlo Kalman filter (SMC-KF)[1] for the IMU-based navigation, which uses a particle filter for nonlinear orientation estimation with a bank of Kalman filters for estimating the remaining states (e.g., position, velocity). The proposed method significantly outperforms the EKF in navigation accuracy.
- We develop a steepest descent random start (SDRS) algorithm for the WiFi RSSI-based radiolocation. The proposed scheme using WiFi RSSI achieves performance close to that of the RTT-based scheme, but with much easier implementation on smartphones.
- We integrate the WiFi RSSI and smartphone inertial sensor measurements in a navigation filter. The simulation results shows that the information fusion provides significant improvements compared with RSSI-only or IMU-only navigation.

II. System Model of Smartphone IMU

In this section, we describe the process model and measurement model of the inertial sensors (i.e., accelerometer and gyroscope) on a smartphone.

We define the orientation of a smartphone as $\boldsymbol{\varphi}(n) = [\varphi_x(n), \varphi_y(n), \varphi_z(n)]^{\mathrm{T}}$, representing the three simultaneous orthogonal rotation angles. The state $\boldsymbol{x}(n)$ contains position, velocity, acceleration, and the derivative of orientation, given

This research was supported, in part, by the National Science Foundation under Grant ECCS-0901034, the Office of Naval Research under Grant N00014-11-1-0397, the Defense University Research Instrumentation Program under Grant N00014-08-1-0826, and the MIT Institute for Soldier Nanotechnologies.

[1]The development of the SMC-KF can be viewed as a Rao-Blackwellized particle filter [19], but the SMC-KF uses the quasi-optimal importance density instead of the suboptimal one-step prediction simulation density used in [14].

by

$$\boldsymbol{x}(n) = [\, x(n),\, y(n),\, z(n),\, \dot{x}(n),\, \dot{y}(n),\, \dot{z}(n),\, \ddot{x}(n),\, \ddot{y}(n),\, \ddot{z}(n),\, \dot{\varphi}_x(n),\, \dot{\varphi}_y(n),\, \dot{\varphi}_z(n)\,]^{\mathrm{T}}.$$

Both $\boldsymbol{\varphi}(n)$ and $\boldsymbol{x}(n)$ are represented with respect to the *reference frame*.

The process model can be written as

$$\boldsymbol{x}(n+1) = \mathbf{F}\boldsymbol{x}(n) + \mathbf{G}\mathbf{w}(n) \tag{1}$$

$$\boldsymbol{\varphi}(n+1) = \boldsymbol{\varphi}(n) + T\dot{\boldsymbol{\varphi}}(n) + \frac{T^2}{2}\mathbf{w}_{\boldsymbol{\varphi}}(n) \tag{2}$$

where

$$\mathbf{F} = \begin{bmatrix} \mathbf{I}_3 & T\mathbf{I}_3 & T^2/2\mathbf{I}_3 & \mathbf{0}_3 \\ \mathbf{0}_3 & \mathbf{I}_3 & T\mathbf{I}_3 & \mathbf{0}_3 \\ \mathbf{0}_3 & \mathbf{0}_3 & \mathbf{I}_3 & \mathbf{0}_3 \\ \mathbf{0}_3 & \mathbf{0}_3 & \mathbf{0}_3 & \mathbf{I}_3 \end{bmatrix},\ \mathbf{G} = \begin{bmatrix} T^3/6\mathbf{I}_3 & \mathbf{0}_3 \\ T^2/2\mathbf{I}_3 & \mathbf{0}_3 \\ T\mathbf{I}_3 & \mathbf{0}_3 \\ \mathbf{0}_3 & T\mathbf{I}_3 \end{bmatrix}$$

with the sample time T, and $\mathbf{I}_k$ and $\mathbf{0}_k$ denoting the $k \times k$ unit matrix and zero matrix, respectively. The noise vector $\mathbf{w}(n) = [\,\mathrm{w}_x(n),\, \mathrm{w}_y(n),\, \mathrm{w}_z(n),\, \mathrm{w}_{\varphi_x}(n)\, \mathrm{w}_{\varphi_y}(n),\, \mathrm{w}_{\varphi_z}(n)]^{\mathrm{T}}$, of which the first three elements model the jerk noise as an i.i.d. Gaussian sequence, i.e., $[\mathrm{w}_x(n),\, \mathrm{w}_y(n),\, \mathrm{w}_z(n)]^{\mathrm{T}} \sim \mathcal{N}(\mathbf{0}, \mathbf{Q})$, and the last three elements model the orientation derivative process noise as $\mathbf{w}_{\boldsymbol{\varphi}}(n) \sim \mathcal{N}(\mathbf{0}, \mathbf{Q}_{\boldsymbol{\varphi}})$. The covariance matrices $\mathbf{Q} = \mathrm{diag}(\sigma_x^2, \sigma_y^2, \sigma_z^2)$ and $\mathbf{Q}_{\boldsymbol{\varphi}} = \mathrm{diag}(\sigma_{\varphi_x}^2, \sigma_{\varphi_y}^2, \sigma_{\varphi_z}^2)$ with standard deviations in m/s^3 and rad/s^2, respectively.

The smartphone inertial sensor measurements include the angular velocity $\boldsymbol{\omega}$ and the force normalized by the constant mass of the IMU $\boldsymbol{f}$, both with respect to the *body frame*. The IMU measurement model is given by

$$\boldsymbol{z}_{\mathrm{IMU}}(n) = \begin{bmatrix} \boldsymbol{\omega}(n) \\ \boldsymbol{f}(n) \end{bmatrix} = \mathbf{H}\big(\boldsymbol{\varphi}(n)\big)\big(\boldsymbol{x}(n) - \boldsymbol{x}_g\big) + \mathbf{v}_{\mathrm{IMU}}(n) \tag{3}$$

where $\boldsymbol{x}_g = [\mathbf{0}_{1\times 8},\, g,\, \mathbf{0}_{1\times 3}]^{\mathrm{T}}$ is the gravity acceleration, and

$$\mathbf{H}\big(\boldsymbol{\varphi}(n)\big) = \begin{bmatrix} \mathbf{0}_3 & \mathbf{0}_3 & \mathbf{0}_3 & \mathbf{C}_1(\boldsymbol{\varphi}(n)) \\ \mathbf{0}_3 & \mathbf{0}_3 & \mathbf{C}_2(\boldsymbol{\varphi}(n)) & \mathbf{0}_3 \end{bmatrix}$$

with matrices $\mathbf{C}_1(\boldsymbol{\varphi}(n)) \in \mathbb{R}^{3\times 3}$ and $\mathbf{C}_2(\boldsymbol{\varphi}(n)) \in \mathbb{R}^{3\times 3}$ given by [9], [20]

$$\begin{aligned} \mathbf{C}_1(\boldsymbol{\varphi}(n)) &= \mathbf{I}_3 - \|\boldsymbol{\varphi}(n)\|^{-2}\big(1 - \cos\|\boldsymbol{\varphi}(n)\|\big)[\boldsymbol{\varphi}(n)]_\times \\ &\quad + \|\boldsymbol{\varphi}(n)\|^{-3}\big(1 - \sin\|\boldsymbol{\varphi}(n)\|/\|\boldsymbol{\varphi}(n)\|\big)[\boldsymbol{\varphi}(n)]_\times^2 \\ \mathbf{C}_2(\boldsymbol{\varphi}(n)) &= \mathbf{I}_3 - \|\boldsymbol{\varphi}(n)\|^{-1}\sin\|\boldsymbol{\varphi}(n)\|[\boldsymbol{\varphi}(n)]_\times \\ &\quad + \|\boldsymbol{\varphi}(n)\|^{-2}\big(1 - \cos\|\boldsymbol{\varphi}(n)\|\big)[\boldsymbol{\varphi}(n)]_\times^2 \end{aligned}$$

and $[\boldsymbol{\varphi}(n)]_\times$ denoting the skew-symmetric form of the vector $\boldsymbol{\varphi}(n)$, i.e.,

$$[\boldsymbol{\varphi}(n)]_\times = \begin{bmatrix} 0 & -\varphi_z & \varphi_y \\ \varphi_z & 0 & -\varphi_x \\ -\varphi_y & \varphi_x & 0 \end{bmatrix}.$$

The additive IMU noise $\mathbf{v}_{\mathrm{IMU}}(n) = [\,\mathbf{v}_{\boldsymbol{\omega}}(n),\, \mathbf{v}_{\boldsymbol{f}}(n)\,]^{\mathrm{T}}$ is an i.i.d. Gaussian sequence with $\mathbf{v}_{\boldsymbol{\omega}}(n) \sim \mathcal{N}(\mathbf{0}, \sigma_{\boldsymbol{\omega}}^2\mathbf{I}_3)$ and $\mathbf{v}_{\boldsymbol{f}}(n) \sim \mathcal{N}(\mathbf{0}, \sigma_{\boldsymbol{f}}^2\mathbf{I}_3)$. The covariance matrix of $\mathbf{v}_{\mathrm{IMU}}(n)$ is denoted as $\mathbf{R}_{\mathrm{IMU}}$.

III. Sequential Monte Carlo Kalman Filter for IMU-based Navigation

In this section, we design a nonlinear filter for the smartphone navigation problem using inertial sensors measurements. Since the measurement model (3) is a nonlinear function of orientation, we apply the sequential importance sampling method to the orientation estimation, while adopting measurement linearization for construction of a practical simulation density. Such method is referred to as SMC-KF [21], [22].

In the SMC-KF, the estimated states are determined by

$$\hat{\boldsymbol{\varphi}}(n) = \sum_{i=1}^{N_{\mathrm{s}}} w^i(n)\boldsymbol{\varphi}^i(n), \quad \hat{\boldsymbol{x}}(n|n) = \sum_{i=1}^{N_{\mathrm{s}}} w^i(n)\hat{\boldsymbol{x}}^i(n|n) \tag{4}$$

where $w^i(n)$ is the weight of the ith particle $\boldsymbol{\varphi}^i(n)$, N_{s} is the number of particles, and $\hat{\boldsymbol{x}}(n|n) = \mathbb{E}\{\boldsymbol{x}(n)|\boldsymbol{z}^n\}$ is the estimated state vector given cumulative measurements $\boldsymbol{z}^n = \{\boldsymbol{z}(l),\ l = 0, \cdots, n\}$.[2]

A. Particle Filter for Estimating $\boldsymbol{\varphi}^i(n)$

Consider a particle filter with N_{s} *particle streams*, i.e.,

$$\boldsymbol{\varphi}^{i,n} \triangleq \{\boldsymbol{\varphi}^i(l),\ l = 0, \cdots, n\}, \quad i = 1, \cdots, N_{\mathrm{s}}.$$

The particles $\boldsymbol{\varphi}^i(n)$ are generated as random samples from the importance sampling density $q(\boldsymbol{\varphi}^i(n)|\boldsymbol{\varphi}^{i,n-1}, \boldsymbol{z}^n)$. The optimal importance density is given by [22]

$$\begin{aligned} &q(\boldsymbol{\varphi}^i(n)|\boldsymbol{\varphi}^{i,n-1}, \boldsymbol{z}^n) \\ &= p(\boldsymbol{\varphi}^i(n)|\boldsymbol{\varphi}^{i,n-1}, \boldsymbol{z}^n) \\ &= \frac{p(\boldsymbol{z}(n)|\boldsymbol{\varphi}^{i,n}, \boldsymbol{z}^{n-1})p(\boldsymbol{\varphi}^i(n)|\boldsymbol{\varphi}^{i,n-1}, \boldsymbol{z}^{n-1})}{p(\boldsymbol{z}(n)|\boldsymbol{\varphi}^{i,n-1}, \boldsymbol{z}^{n-1})} \\ &= \frac{1}{c^i}\mathcal{N}\Big(\boldsymbol{z}(n); \mathbf{H}\big(\boldsymbol{\varphi}^i(n)\big)\big(\hat{\boldsymbol{x}}^i(n|n-1) - \boldsymbol{x}_g\big), \\ &\qquad \mathbf{H}\big(\boldsymbol{\varphi}^i(n)\big)\mathbf{P}^i(n|n-1)\mathbf{H}\big(\boldsymbol{\varphi}^i(n)\big)^{\mathrm{T}} + \mathbf{R}\Big) \\ &\cdot\mathcal{N}\Big(\boldsymbol{\varphi}^i(n-1) + T\hat{\dot{\boldsymbol{\varphi}}}^i(n|n-1), T^2\mathbf{P}^i_{\dot{\boldsymbol{\varphi}}}(n|n-1) + T^4/4\mathbf{Q}_{\boldsymbol{\varphi}}\Big) \end{aligned} \tag{5}$$

where $c^i = p(\boldsymbol{z}(n)|\boldsymbol{\varphi}^{i,n-1}, \boldsymbol{z}^{n-1})$ is a constant with respect to $\boldsymbol{\varphi}^i(n)$, and $\hat{\boldsymbol{x}}^i(n|n-1) = \mathbb{E}\{\boldsymbol{x}^i(n)|\boldsymbol{\varphi}^{i,n-1}, \boldsymbol{z}^{n-1}\}$. The nonlinearity of $\mathbf{H}\big(\boldsymbol{\varphi}^i(n)\big)$ precludes combining the product of Gaussian densities in (5) into a single Gaussian, hence obtaining a tractable sampling distribution. To address the problem, we adopt the SMC-KF [21] to approximate the importance density. Specifically, we perform the following linearization approximation in (5):

$$\begin{aligned} &\mathbf{H}\big(\boldsymbol{\varphi}^i(n)\big)\big(\hat{\boldsymbol{x}}^i(n|n-1) - \boldsymbol{x}_g\big) \\ &\approx \mathbf{H}\big(\widetilde{\boldsymbol{\varphi}}^i(n)\big)\big(\hat{\boldsymbol{x}}^i(n|n-1) - \boldsymbol{x}_g\big) + \mathbf{J}^i(n)\big(\boldsymbol{\varphi}^i(n) - \widetilde{\boldsymbol{\varphi}}^i(n)\big) \end{aligned} \tag{6}$$

$$\begin{aligned} &\mathbf{H}\big(\boldsymbol{\varphi}^i(n)\big)\mathbf{P}^i(n|n-1)\mathbf{H}\big(\boldsymbol{\varphi}^i(n)\big)^{\mathrm{T}} + \mathbf{R} \\ &\approx \mathbf{H}\big(\widetilde{\boldsymbol{\varphi}}^i(n)\big)\mathbf{P}^i(n|n-1)\mathbf{H}\big(\widetilde{\boldsymbol{\varphi}}^i(n)\big)^{\mathrm{T}} + \mathbf{R} \\ &\triangleq \boldsymbol{\Sigma}^i(n|n-1) \end{aligned} \tag{7}$$

[2]For notation simplicity, we omit the subscript "IMU" in this section.

where $\widetilde{\boldsymbol{\varphi}}^i(n) = \boldsymbol{\varphi}^i(n-1) + T\hat{\dot{\boldsymbol{\varphi}}}^i(n|n-1)$, and $\mathbf{J}^i(n) \in \mathbb{R}^{6\times 3}$ is the Jacobian matrix given by

$$\mathbf{J}^i(n) = \frac{\partial \mathbf{H}(\boldsymbol{\varphi}(n))\big(\hat{\boldsymbol{x}}^i(n|n-1) - \boldsymbol{x}_g\big)}{\partial \boldsymbol{\varphi}(n)}\Big|_{\boldsymbol{\varphi}(n)=\widetilde{\boldsymbol{\varphi}}^i(n)}.$$

Note that the linearization of $\mathbf{H}\big(\boldsymbol{\varphi}^i(n)\big)$ and $\mathbf{J}^i(n)$ are evaluated at $\widetilde{\boldsymbol{\varphi}}^i(n) = \boldsymbol{\varphi}^i(n-1) + T\hat{\dot{\boldsymbol{\varphi}}}^i(n|n-1)$, since $\widetilde{\boldsymbol{\varphi}}^i(n)$ is more accurate than $\boldsymbol{\varphi}^i(n-1)$ and thus can help to reduce the linearization error. Substitution of (6) and (7) into (5) yields the following proposition.

Proposition 1: The density $p(\boldsymbol{\varphi}^i(n)|\boldsymbol{\varphi}^{i,n-1}, \boldsymbol{z}^n)$ can be approximated as a single Gaussian distribution using the linearization in (6) and (7):

$$p(\boldsymbol{\varphi}^i(n)|\boldsymbol{\varphi}^{i,n-1}, \boldsymbol{z}^n) = \mathcal{N}(\boldsymbol{\varphi}^i(n); \overline{\boldsymbol{\varphi}}^i(n), \mathbf{P}^i_{\boldsymbol{\varphi}}(n)) \quad (8)$$

where

$$\begin{aligned}\overline{\boldsymbol{\varphi}}^i(n) &= \widetilde{\boldsymbol{\varphi}}^i(n) + \mathbf{P}^i_{\boldsymbol{\varphi}}(n)\mathbf{J}^i(n)^{\mathrm{T}}\boldsymbol{\Sigma}^i(n|n-1)^{-1} \\ &\quad \cdot \big(\boldsymbol{z}(n) - \mathbf{H}(\widetilde{\boldsymbol{\varphi}}^i(n))\big(\hat{\boldsymbol{x}}^i(n|n-1) - \boldsymbol{x}_g\big)\big) \\ \mathbf{P}^i_{\boldsymbol{\varphi}}(n)^{-1} &= \mathbf{J}^i(n)^{\mathrm{T}}\boldsymbol{\Sigma}^i(n|n-1)^{-1}\mathbf{J}^i(n) \\ &\quad + \big(T^2\mathbf{P}^i_{\dot{\boldsymbol{\varphi}}}(n|n-1) + T^4/4\mathbf{Q}_{\boldsymbol{\varphi}}\big)^{-1}.\end{aligned}$$

Proof: The derivations follows the standard EKF derivation [22], [23]. Due to the limited space, we omit the details here. □

The recursive weight update is given by

$$w^i(n) \triangleq \frac{p(\boldsymbol{\varphi}^{i,n}|\boldsymbol{z}^n)}{q(\boldsymbol{\varphi}^{i,n}|\boldsymbol{z}^n)} = \frac{p(\boldsymbol{z}(n)|\boldsymbol{\varphi}^{i,n-1}, \boldsymbol{z}^{n-1})}{p(\boldsymbol{z}(n)|\boldsymbol{z}^{n-1})} \cdot w^i(n-1).$$

Since $p\big(\boldsymbol{z}(n)|\boldsymbol{z}^{n-1}\big)$ is a constant and can be omitted after the normalization, we only need to determine the density $p(\boldsymbol{z}(n)|\boldsymbol{\varphi}^{i,n-1}, \boldsymbol{z}^{n-1})$. It can be written as

$$\begin{aligned}&p(\boldsymbol{z}(n)|\boldsymbol{\varphi}^{i,n-1}, \boldsymbol{z}^{n-1}) \\ &= \int p(\boldsymbol{z}(n)|\boldsymbol{\varphi}^{i,n}, \boldsymbol{z}^{n-1}) p(\boldsymbol{\varphi}^i(n)|\boldsymbol{\varphi}^{i,n-1}, \boldsymbol{z}^{n-1}) d\boldsymbol{\varphi}^i(n).\end{aligned}$$

The densities in the above equation have been derived in (5). Using the linearization in (6) and (7), we have

$$\begin{aligned}&p(\boldsymbol{z}(n)|\boldsymbol{\varphi}^{i,n-1}, \boldsymbol{z}^{n-1}) \\ &= \mathcal{N}\Big(\boldsymbol{z}(n); \mathbf{H}(\widetilde{\boldsymbol{\varphi}}^i(n))\big(\hat{\boldsymbol{x}}^i(n|n-1) - \boldsymbol{x}_g\big), \boldsymbol{\Sigma}^i(n|n-1) \\ &\quad + \mathbf{J}^i(n)\big(T^2\mathbf{P}^i_{\dot{\boldsymbol{\varphi}}}(n|n-1) + T^4/4\mathbf{Q}_{\boldsymbol{\varphi}}\big)\mathbf{J}^i(n)^{\mathrm{T}}\Big).\end{aligned}$$

Hence, the weight update is given by

$$w^i(n) = \frac{1}{c}\, p(\boldsymbol{z}(n)|\boldsymbol{\varphi}^{i,n-1}, \boldsymbol{z}^{n-1}) \cdot w^i(n-1) \quad (9)$$

where c is a normalization constant.

B. Kalman Filter for Estimating Non-Orientation States

The non-orientation state processes including position, velocity, acceleration, and angle derivative along with their measurements can be modeled as linear Gaussian, once the orientation is specified. Hence, the Kalman filter is optimal for estimating $\boldsymbol{x}(n)$ given the particle stream $\boldsymbol{\varphi}^{i,n}$. Specifically, we use N_{s} parallel Kalman filters to estimate $\hat{\boldsymbol{x}}^i(n)$, $i = 1, \cdots, N_{\mathrm{s}}$.

Algorithm 1 SMC-KF Algorithm for IMU-based Navigation

Given: $\boldsymbol{\varphi}^i(n-1)$, $\hat{\boldsymbol{x}}^i(n|n-1)$, $\mathbf{P}^i(n|n-1)$ and the IMU measurement $\boldsymbol{z}_{\mathrm{IMU}}(n)$

for $i = 1, \cdots, N_{\mathrm{s}}$ **do** ▷ SMC Filter
  Generate particle $\boldsymbol{\varphi}^i(n) \sim p(\boldsymbol{\varphi}^i(n)|\boldsymbol{\varphi}^{i,n-1}, \boldsymbol{z}^n)$ via (8)
  Update weight $w^i(n)$ via (9)
end for
Normalize weights $\widetilde{w}^i(n) = w^i(n)/\sum_{i=1}^{N_{\mathrm{s}}} w^i(n)$, $\forall i$
Calculate effective sample size $\widehat{N}_{\mathrm{eff}} = 1/\sum_{i=1}^{N_{\mathrm{s}}}(\widetilde{w}^i(n))^2$
if $\widehat{N}_{\mathrm{eff}} \le N_{\mathrm{T}}$ **then**
  Systematical resampling (cf. [7]) of $\boldsymbol{\varphi}^i(n)$, and set $w^i(n) = 1/N_{\mathrm{s}}$
end if
for $i = 1, \cdots, N_{\mathrm{s}}$ **do** ▷ Kalman Filter
  Update $\hat{\boldsymbol{x}}^i(n|n)$ and $\mathbf{P}^i(n|n)$ via (10)–(12)
  Predict $\hat{\boldsymbol{x}}^i(n+1|n)$ and $\mathbf{P}^i(n+1|n)$ via (13)–(14)
end for
Calculate the estimated states $\hat{\boldsymbol{\varphi}}(n)$ and $\hat{\boldsymbol{x}}(n|n)$ via (4).

The Kalman filter gain is given by

$$\begin{aligned}\mathbf{K}^i(n) &= \mathbf{P}^i(n|n-1)\mathbf{H}^{\mathrm{T}}(\boldsymbol{\varphi}^i(n)) \\ &\quad \cdot \big(\mathbf{H}(\boldsymbol{\varphi}^i(n))\mathbf{P}^i(n|n-1)\mathbf{H}^{\mathrm{T}}(\boldsymbol{\varphi}^i(n)) + \mathbf{R}\big)^{-1}. \quad (10)\end{aligned}$$

The correction steps are given by

$$\begin{aligned}\hat{\boldsymbol{x}}^i(n|n) &= \hat{\boldsymbol{x}}^i(n|n-1) + \mathbf{K}^i(n) \\ &\quad \cdot \big(\boldsymbol{z}(n) - \mathbf{H}(\boldsymbol{\varphi}^i(n))\big(\hat{\boldsymbol{x}}^i(n|n-1) - \boldsymbol{x}_g\big)\big) \quad (11) \\ \mathbf{P}^i(n|n) &= \big(\mathbf{I} - \mathbf{K}^i(n)\mathbf{H}(\boldsymbol{\varphi}^i(n))\big)\mathbf{P}^i(n|n-1). \quad (12)\end{aligned}$$

The prediction steps are given by

$$\begin{aligned}\hat{\boldsymbol{x}}^i(n+1|n) &= \mathbf{F}\hat{\boldsymbol{x}}^i(n|n) \quad (13) \\ \mathbf{P}^i(n+1|n) &= \mathbf{F}\mathbf{P}^i(n|n)\mathbf{F}^{\mathrm{T}} + \mathbf{G}\mathbf{Q}\mathbf{G}^{\mathrm{T}}. \quad (14)\end{aligned}$$

The overall SMC-KF algorithm for IMU-based navigation is described in Algorithm 1.

IV. Radiolocation Using WiFi RSSI

In addition to the inertial sensor measurements, WiFi signals can be exploited in smartphone navigation due to the ever increasing density of WiFi networks.. In this section, we develop a radiolocation algorithm that infers the smartphone location based on WiFi RSSI measurements.

A. Steepest Descent Random Start (SDRS) Positioning Algorithm

We consider a scenario in which a single static smartphone computes its position using the RSSI from adjacent wireless access points (AP). The smartphone obtains RSSI measurement in dBm $z_{\mathrm{RSSI},j}$ from access point (AP) j, given by [24]

$$z_{\mathrm{RSSI},j}(n) = s^{\mathrm{a}}_j - 10\eta_j \log_{10}\frac{||\mathbf{p}(n) - \mathbf{p}^{\mathrm{a}}_j||}{d_0} + v_j(n),\ \forall j \in \mathcal{N}_{\mathrm{a}}$$

where s_j^{a} is the AP transmit power in dBm, η_j is the path loss exponent, $\mathbf{p}(n)$ and $\mathbf{p}_j^{\text{a}}$ are the positions of the smartphone and the APs, respectively, d_0 is the reference distance, $v_j(n)$ is the measurement noise, and $\mathcal{N}_{\text{a}}$ is the set of adjacent APs. For Gaussian noise $v_j(n)$, the maximum-likelihood position estimate corresponds to the minimum of the objective function

$$f(\mathbf{p}(n)) = \sum_{j\in\mathcal{N}_{\text{a}}} \Big(z_{\text{RSSI},j}(n) - s_j^{\text{a}} + 10\eta_j \log_{10} \frac{||\mathbf{p}(n) - \mathbf{p}_j^{\text{a}}||}{d_0} \Big)^2.$$

The SDRS algorithm uses multiple initial starting points $\mathbf{p}^{q,0},\ q = 1, \cdots, N_{\text{start}}$ uniformly distributed in the scenario region. The N_{start} points are processed in parallel with l_q iterations at which convergence is declared. The SDRS estimate corresponds to $\hat{\mathbf{p}} = \mathbf{p}^{q^*,l_{q^*}}$, where $q^* = \arg\min_q f(\mathbf{p}^{q,l_q})$. The SDRS algorithm can be interpreted as a lightweight particle filter, in which the random start positions $\mathbf{p}^{q,0}$ correspond to an initial choice of particles, and with a single particle $\hat{\mathbf{p}}$ surviving at the end of the algorithm. The description of the SDRS algorithm can be referred to [25].

B. Path Loss Exponent Decision

The accuracy of SDRS algorithm relies on the path loss exponent η_j. Since the path loss exponent changes fairly slowly for the pedestrian applications here, e.g., LOS or NLOS, we consider two hypotheses of the path loss exponent as $\{\text{LOS}: \ \eta_j = 2\}$ and $\{\text{NLOS}: \ \eta_j = 4\}$.[3] Then we apply a *binary decision rule* using multiple RSSI measurements to determine the path loss exponent. We let $\boldsymbol{z}_{\text{RSSI},j}(n) = \{z_{\text{RSSI},j}(l),\ l \in \mathcal{N}_{\text{RSSI}}(n)\}$ denote the N_{RSSI} adjacent independent RSSI measurements, i.e., $\mathcal{N}_{\text{RSSI}}(n) = \{n - N_{\text{RSSI}} + 1, n - N_{\text{RSSI}} + 2, \cdots, n\}$. Given $v_j \sim \mathcal{N}(0, \sigma^2)$, the likelihood ratio can be derived as

$$\frac{f(\boldsymbol{z}_{\text{RSSI},j}(n)|\text{NLOS})}{f(\boldsymbol{z}_{\text{RSSI},j}(n)|\text{LOS})} = \exp\Bigg(-\frac{1}{\sigma^2} \sum_{n\in\mathcal{N}_{\text{RSSI}}} 20\log_{10}\frac{||\hat{\mathbf{p}}(n|n) - \mathbf{p}_j^{\text{a}}||}{d_0} \cdot \Big(z_j(n) - s_j^{\text{a}} + 30\log_{10}\frac{||\hat{\mathbf{p}}(n|n) - \mathbf{p}_j^{\text{a}}||}{d_0} \Big) \Bigg).$$

The decision rule is given by

$$\frac{f(\boldsymbol{z}_{\text{RSSI},j}(n)|\text{NLOS})}{f(\boldsymbol{z}_{\text{RSSI},j}(n)|\text{LOS})} \underset{\text{LOS}}{\overset{\text{NLOS}}{\gtrless}} \lambda$$

where λ is a threshold. It follows that

$$g(\boldsymbol{z}_{\text{RSSI},j}(n)) \underset{\text{NLOS}}{\overset{\text{LOS}}{\lessgtr}} \gamma_{\text{th}} = -\sigma^2 \ln\lambda \tag{15}$$

where

$$g(\boldsymbol{z}_{\text{RSSI},j}(n)) = \sum_{n\in\mathcal{N}_{\text{RSSI}}} 20\log_{10}\frac{||\hat{\mathbf{p}}(n|n) - \mathbf{p}_j^{\text{a}}||}{d_0} \cdot \Big(z_j(n) - s_j^{\text{a}} + 30\log_{10}\frac{||\hat{\mathbf{p}}(n|n) - \mathbf{p}_j^{\text{a}}||}{d_0} \Big).$$

The threshold λ is given by

$$\lambda = \frac{p_{\text{LOS}}(C_{\text{NLOS|LOS}} - C_{\text{LOS|LOS}})}{p_{\text{NLOS}}(C_{\text{LOS|NLOS}} - C_{\text{NLOS|NLOS}})}$$

[3] A more complicated algorithm considering continuous η_j is given in [18].

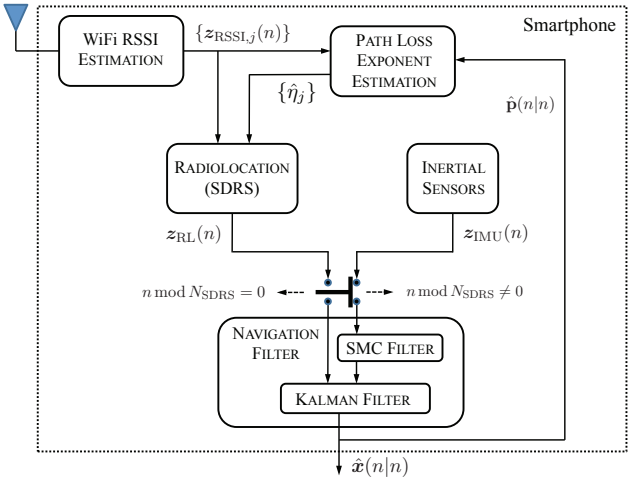

Fig. 1: Smartphone navigation system with information fusion of WiFi RSSI and inertial sensor measurements.

where $C_{\text{H|K}}$ is the cost of detecting H when K is true. Assume equal prior probability $p_{\text{LOS}} = p_{\text{NLOS}} = 1/2$, and the cost $C_{\text{LOS|LOS}} = C_{\text{NLOS|NLOS}} = 0$, $C_{\text{LOS|NLOS}} = C_{\text{NLOS|LOS}}$, we have $\lambda = 1$.

C. Kalman Filter for SDRS Position Estimate

To track the smartphone location, the SDRS estimates are further treated as linear Gaussian measurements by a Kalman filter. Specifically, we consider the process model (1). The measurement model is written as

$$\boldsymbol{z}_{\text{RL}}(n) = \mathbf{H}_{\text{RL}}(n)\boldsymbol{x}(n) + \boldsymbol{v}_{\text{RL}}(n),\ n \bmod N_{\text{SDRS}} = 0$$

where $\mathbf{H}_{\text{RL}} = [\mathbf{I}_3\ \mathbf{0}_3\ \mathbf{0}_3\ \mathbf{0}_3]$, and the SDRS position estimation error is taken to be Gaussian, i.e., $\boldsymbol{v}_{\text{RL}} \sim \mathcal{N}(\mathbf{0}, \sigma_{\text{RL}}^2\mathbf{I}_3)$. The covariance matrix of $\mathbf{v}_{\text{RL}}(n)$ is denoted as $\mathbf{R}_{\text{RL}}$. The details of the Kalman filter is similar to Sec. III-B.

V. Information Fusion in Smartphone Navigation

In this section, we propose a smartphone navigation system which fuses the WiFi RSSI and inertial sensor measurements. The system diagram is shown in Fig. 1. The specific blocks perform the following tasks:

- *WiFi RSSI Estimation:* it includes a WiFi module that obtains RSSI measurements $\boldsymbol{z}_{\text{RSSI},j}(n)$ from the in-range APs $j \in \mathcal{N}_a$.
- *Path Loss Exponent Estimation:* it performs a binary decision (Sec. IV-B) on path loss exponent η_j based on multiple RSSI measurements $\{\boldsymbol{z}_{\text{RSSI},j}(n)\}$. Moreover, the binary decision of η_j also requires the estimated position. Since η_j varies slowly during normal walking, the binary decision is not very sensitive to the position estimation error. Hence, we directly use the estimated position $\hat{\mathbf{p}}(n|n)$ obtained from the navigation filter.
- *Radiolocation (SDRS):* runs the SDRS algorithm (Sec. IV-A) to infer the smartphone position based on RSSI measurements $\boldsymbol{z}_{\text{RSSI},j}(n),\ j \in \mathcal{N}_a$.

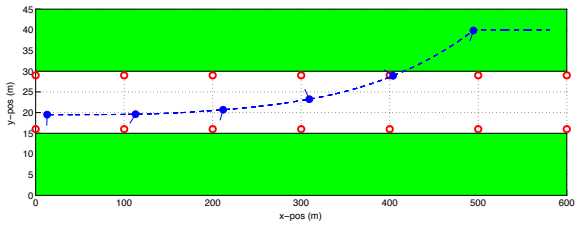

Fig. 2: The urban corridor with a single mobile node trajectory.

- *Inertial Sensors:* contain 3-D accelerometer and 3-D gyroscope, which measure the acceleration and angular velocity with respect to the body frame. The IMU model is described in Sec. II.
- *Navigation Filter:* fuses the SMC-KF (Sec. III) for inertial sensor measurements and the Kalman filter (Sec. III-B) for radiolocation. We assume that SDRS algorithm position estimates are computed after every N_{SDRS} IMU measurements. The SDRS estimates are treated as linear Gaussian measurements by a Kalman filter when $n \mod N_{\text{SDRS}} = 0$. The IMU measurements are treated as nonlinear Gaussian measurements by the SMC-KF when $n \mod N_{\text{SDRS}} \neq 0$.

VI. Simulation Results

In this section, we simulate the WiFi RSSI and IMU based smartphone navigation algorithm in a 2-D urban corridor scenario.

The urban corridor is illustrated in Fig. 2, where the street is 15 m wide with buildings 15 m wide on the north and south sides. Fourteen WiFi APs (red rings) are placed in two rows along the corridor, separated by every 100 m. A single mobile node (blue dots) moves according to the Gaussian acceleration model in (1)-(2) at a nominal velocity of 1 m/s heading east, and gradually moves into the buildings on two sides. The mobile node is also rotating itself, with random initial orientation φ_z in $[-\pi, \pi]$. The small bar on the blue dot denotes the orientation of mobile node. RSSI measurements z_j are assumed to be LOS ($\sigma = 4$ dB) when the mobile node is in the street, otherwise the measurements are modeled as NLOS ($\sigma = 10$ dB) [24]. The simulation parameters are summarized in Table I.

In Fig. 3, we first investigate the performance of information fusion in the smartphone navigation. Specifically, we plot the average position estimation errors along the time axis, and compare the scheme using information fusion with the ones using RSSI measurements or inertial sensor measurements only.[4] It shows that using IMU only fails to track the smartphone position over the long term. The RSSI-only scheme is able to track the movement but with fairly large position error, i.e., 22.59 m on average. The fusion of both RSSI and IMU measurements reduces the position error to 7.83 m on average, which is 65% lower compared with the RSSI-only schemes.

[4]We adopt the Kalman filter in the RSSI-only scheme and the SMC-KF in the IMU-only scheme.

Jerk noise standard deviation (STD): σ	1e-1 m/s^3
Angular acceleration noise STD: σ_φ	5e-1 rad/s^2
IMU gyro (angular velocity) noise STD: σ_ω	5.2e-4 rad/s
IMU accelerometer (force) noise STD: σ_f	2e-3 m/s$^2/\sqrt{\text{Hz}}$
AP-to-mobile communication range	100 m
AP transmit power: s_j^a	15 dBm
Reference distance: d_0	1 m
SDRS position estimation error STD: σ_{RL}	1.5 m
Number of particles: N_s	8
Number of random starting points for SDRS	8
Number of IMU updates per SDRS update: N_{SDRS}	100
Sample time: T	0.1 sec
Total simulation duration	600 sec
Number of simulation runs for error averaging	100

TABLE I: Urban corridor simulation parameters

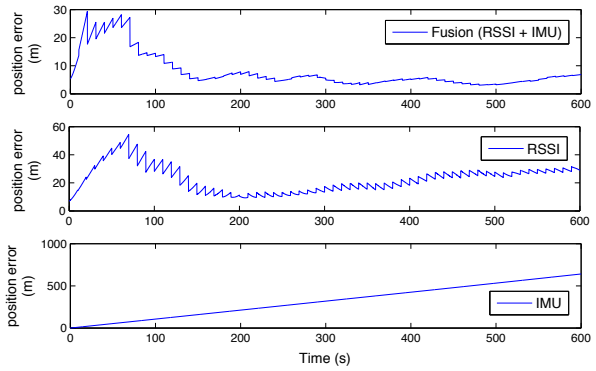

Fig. 3: Information fusion improves the navigation accuracy.

Hence, it confirms the importance of the information fusion in location tracking.

In Fig. 4, we compare the performance of the SMC-KF with the conventional EKF. Specifically, we plot the cumulative density function (CDF) curve of the position and angle estimation errors. It shows that the SMC-KF significantly outperforms the EKF. The position error of SMC-KF is 13 m lower than that of EKF with 80% probability. On average, the position error is reduced by 60%. Moreover, the angle estimation using SMC-KF is improved by 0.13 rads with 80% probability compared with that using EKF. On average, the angle error is reduced by 83%. This is mainly because the SMC-KF uses multiple particles to estimate the angles, which results in lower estimation errors compared with a single EKF.

In Fig. 5, we compare the proposed system using WiFi RSSI and the system using UWB radio round trip time (RTT) measurements in [14]. Both systems exploit inertial sensors for the orientation estimation. Hence, the angle estimation errors are similar. Due to the fine resolution of UWB signals, its RTT measurements provides much more precise location accuracy. As shown in the figure, the position error using RTT measurements is 4.4 m lower with 80% probability, and the gap is up to 3.1 m with 50% probability. Despite the higher error of RSSI versus UWB navigation, the former's low cost and wide availability makes the performance tradeoff acceptable.

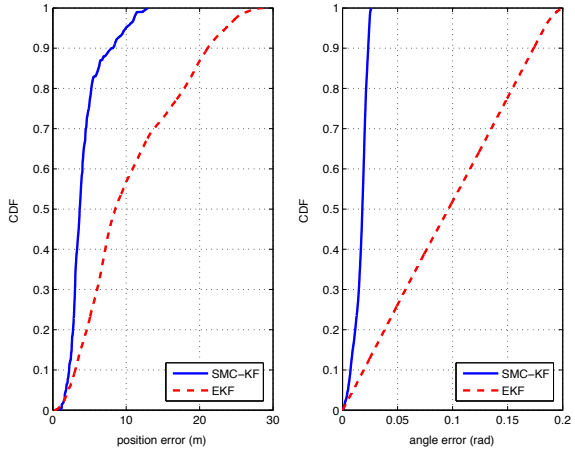

Fig. 4: SMC-KF achieves higher location accuracy compared with EKF in IMU-based navigation.

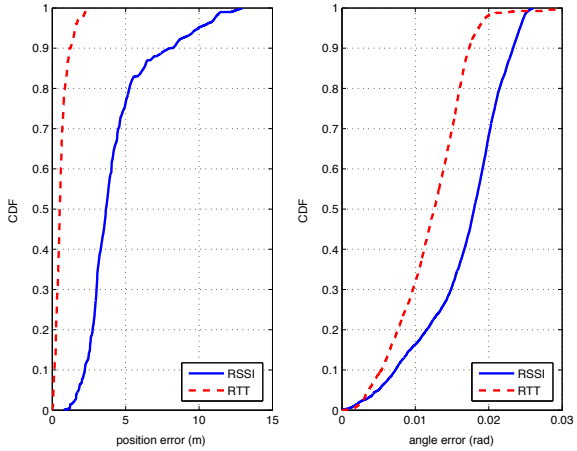

Fig. 5: WiFi RSSI achieves useable accuracy compared with UWB RTT in the fusion with IMU measurements.

VII. Conclusion

In this paper, we proposed a location tracking algorithm that fuses WiFi RSSI and smartphone IMU measurements. The nonlinear IMU measurements are processed by a SMC-KF, and then integrated with the radiolocation information inferred from WiFi RSSI. An urban corridor simulation shows that the fusion algorithm with SMC-KF reduces the position error by 13 m with 80% probability compared with the conventional EKF. Moreover, it shows that the information fusion achieves 65% lower position error compared with the navigation scheme without using smartphone inertial sensors.

References

[1] M. Z. Win, A. Conti, S. Mazuelas, Y. Shen, W. M. Gifford, D. Dardari, and M. Chiani, "Network localization and navigation via cooperation," *IEEE Commun. Mag.*, vol. 49, no. 5, pp. 56–62, May 2011.

[2] K. Pahlavan, X. Li, and J.-P. Mäkelä, "Indoor geolocation science and technology," *IEEE Commun. Mag.*, vol. 40, no. 2, pp. 112–118, Feb. 2002.

[3] Y. Shen, S. Mazuelas, and M. Z. Win, "Network navigation: Theory and interpretation," *IEEE J. Sel. Areas Commun.*, vol. 30, no. 9, pp. 1823–1834, Oct. 2012.

[4] M. Z. Win and R. A. Scholtz, "Ultra-wide bandwidth time-hopping spread-spectrum impulse radio for wireless multiple-access communications," *IEEE Trans. Commun.*, vol. 48, no. 4, pp. 679–691, Apr. 2000.

[5] S. Gezici, Z. Tian, G. B. Giannakis, H. Kobayashi, A. F. Molisch, H. V. Poor, and Z. Sahinoglu, "Localization via ultra-wideband radios: A look at positioning aspects for future sensor networks," *IEEE Signal Process. Mag.*, vol. 22, no. 4, pp. 70–84, Jul. 2005.

[6] D. Dardari, A. Conti, U. J. Ferner, A. Giorgetti, and M. Z. Win, "Ranging with ultrawide bandwidth signals in multipath environments," *Proc. IEEE*, vol. 97, no. 2, pp. 404–426, Feb. 2009.

[7] M. S. Arulampalam, S. Maskell, N. Gordon, and T. Clapp, "A tutorial on particle filters for online nonlinear/non-Gaussian Bayesian tracking," *IEEE Trans. Signal Process.*, vol. 50, no. 2, pp. 174–188, Feb. 2002.

[8] F. Gustafsson, F. Gunnarsson, N. Bergman, U. Forsell, J. Jansson, R. Karlsson, and P. J. Nordlund, "Particle filters for positioning, navigation and tracking," *IEEE Trans. Signal Process.*, vol. 50, no. 2, pp. 425–437, Feb. 2002.

[9] S. Mazuelas, Y. Shen, and M. Z. Win, "Belief condensation filtering," *IEEE Trans. Signal Process.*, 2013, to appear.

[10] E. Foxlin, "Pedestrian tracking with shoe-mounted inertial sensors," *IEEE Comput. Graph. Appl.*, vol. 25, no. 6, pp. 38–46, Nov.-Dec. 2005.

[11] H. Liu, H. Darabi, P. Banerjee, and J. Liu, "Survey of wireless indoor positioning techniques and systems," *IEEE Trans. Syst., Man, Cybern. C*, vol. 37, no. 6, pp. 1067–1086, Nov. 2007.

[12] A. R. Jiménez, F. Seco, J. C. Prieto, and J. Guevara, "Accurate pedestrian indoor navigation by tightly coupling foot-mounted IMU and RFID measurements," *IEEE Trans. Instrum. Meas.*, vol. 61, no. 1, pp. 178 – 189, Jan. 2012.

[13] J. Han, E. Owusu, L. T. Nguyen, A. Perrig, and J. Zhang, "ACComplice: Location inference using accelerometers on smartphones," in *Proc. Int. Conf. on Commun. Syst. and Netw.*, Bangalore, India, Jan. 2012, pp. 1–9.

[14] W. W.-L. Li, R. A. Iltis, and M. Z. Win, "Integrated IMU and radiolocation-based navigation using a Rao-Blackwellized particle filter," in *Proc. IEEE Int. Conf. Acoustics, Speech, and Signal Processing*, Vancouver, Canada, May 2013, pp. 1–5.

[15] Y. Shen and M. Z. Win, "Fundamental limits of wideband localization – Part I: A general framework," *IEEE Trans. Inf. Theory*, vol. 56, no. 10, pp. 4956–4980, Oct. 2010.

[16] F. Evennou and F. Marx, "Advanced Integration of WiFi and Inertial Navigation Systems for Indoor Mobile Positioning," *EURASIP J. Appl. Signal Process.*, pp. 1–11, 2006.

[17] S. M. Siddiqi, G. S. Sukhatme, and A. Howard, "Experiments in Monte-Carlo localization using WiFi signal strength," in *Proc. Int. Conf. Adv. Robot*, Combra, Portugal, Jul. 2003, pp. 210–223.

[18] S. Mazuelas, A. Bahillo, R. Lorenzo, P. Fernandez, F. A. Lago, E. Garcia, J. Blas, and E. Abril, "Robust indoor positioning provided by real-time RSSI values in unmodified WLAN networks," *IEEE J. Sel. Topics Signal Process.*, vol. 3, no. 5, pp. 821–831, Oct. 2009.

[19] B. Ristic, M. S. Arulampalam, and N. Gordon, *Beyond the Kalman Filter: Particle Filters for Tracking Applications*. Norwood, MA: Artech House, 2004.

[20] J. Bortz, "A new mathematical formulation for strapdown inertial navigation," *IEEE Trans. Aerosp. Electron. Syst.*, vol. 7, no. 1, pp. 61 –66, Jan. 1971.

[21] A. Doucet, S. Godsill, and C. Andrieu, "On sequential Monte Carlo sampling methods for bayesian filtering," *Stat. Comput.*, vol. 10, no. 3, pp. 197–208, 2000.

[22] R. A. Iltis, "A sequential Monte Carlo Filter for joint linear/nonlinear state estimation with application to DS-CDMA," *IEEE Trans. Signal Process.*, vol. 51, no. 2, pp. 417–426, Feb. 2003.

[23] B. D. Anderson and J. B. Moore, *Optimal Filtering*. New Jersey: Prentice-Hall, 1979.

[24] A. F. Molisch, *Wireless Communications*, 1st ed. Piscataway, New Jersey, 08855-1331: IEEE Press, J. Wiley and Sons, 2005.

[25] R. A. Iltis, "System-level algorithm design for radionavigation using UWB waveforms," in *Proc. Int. Telemetering Conf.*, San Diego, CA, Oct. 2012, pp. 1–10. [Online]. Available: http://www.ece.ucsb.edu/stnlabs/pubs/navitc12.pdf